W. Gieseke and G. Lange**

Yield Surfaces and Dislocation Structures of Al–3Mg and Copper after Biaxial Cyclic Loadings

REFERENCE Gieseke, W. and Lange, G., **Yield surfaces and dislocation structures of Al–3Mg and copper after biaxial cyclic loadings**, *Multiaxial Fatigue and Design*, ESIS 21 (Edited by A. Pineau, G. Cailletaud, and T. C. Lindley) 1996, Mechanical Engineering Publications, London, pp. 61–74.

ABSTRACT In this paper yield surfaces and dislocation structures are investigated subsequent to plastic cyclic loadings, which were generated as push/pull, alternating torsion, the synchronic superposition of push/pull and alternating torsion, and by 90° phase shifts between push/pull and alternating torsion. With expermiments where the direction of the cyclic loading was changed from push/pull to alternating torsion (and vice versa), it is shown that the anisotropies in the yield surfaces measured with small plastic offset strains after proportional loadings are caused by anisotropies in the dislocation structures and not by the influence of residual stresses.

1 Introduction

Yield surfaces play an important role in many models that simulate the plastic stress/strain behaviour. For example in the two-surface models the interaction of the yield surface with a second, the yield surface always surrounding surface, the so-called bounding surface (**1**, **2**) or memory surface (**3**) is drawn near. Both surfaces in the models are assumed to be von Mises-shaped ellipses. From measurements after unidirectional preloadings it is known, however, that the yield surface measured with small offset strains are characteristically deformed under load (**4**, **5**). In the present work we show the extent to which such yield surface deformations also occur after different cyclic histories. In particular, the influence of the dislocation structure and the influence of residual stresses on the shape of the yield surfaces is discussed.

2 Experimental Details

2.1 *The materials used and the shape of the specimens*

The Al–3Mg (Al + 3wt% Mg) samples were annealed for 6 h at 330°C and then rapidly cooled in water. After this treatment the specimens were completely

*Institut fur Werkstoffe, Technischen Universität Braunschweig, Germany.

recrystallized as a one-phase material with an average grain diameter of 50 μm in all directions. They had a weak ⟨100⟩-fibre texture which remains unchanged during cyclic deformation. It is shown (6) that the yield surface of the virgin material is isotropic, independent of the plastic offset strain used. So it can be concluded that the weak texture has no influence on the saturation yield surfaces discussed here.

The copper specimens were annealed for 4 h at 600°C and then cooled in the furnace. Afterwards the samples were totally recrystallized with an average isotropic grain diameter of 80 μm. The specimens had nearly no texture, so also in the case of copper the texture has no influence on the yield surfaces.

Al–Mg3 had a purity of 99.88% (0.12% other elements than Al and Mg) and copper of 99.99%. Hollow specimens were used as samples with an outer diameter of 28 mm and 2 mm wall thickness in the section of measurement. The length of this section was 40 mm.

2.2 *Methods of measurement*

Proportional cyclic loadings were push/pull, alternating torsion and the synchronic superposition of both. Non-proportional cyclic loadings were generated by 90° phase shifts between push/pull and alternating torsion. Full details about the home-built torsion cylinder and about the home-built strain gauge can be found in reference (6).

The cyclic experiments were controlled by the amplitude of total strain. The given signal was triangular. The equivalent strains were calculated using von Mises criterion with the following relation

$$\varepsilon_{eq} = \left(\varepsilon^2 + \frac{1}{3}\gamma^2\right)^{1/2} \tag{1a}$$

with

$$|\varepsilon| \frac{1}{\sqrt{3}} |\gamma| \tag{1b}$$

where ε is the axial strain while γ is the shear strain. In all experiments the strain rate was 2×10^{-3} s^{-1}. All results presented here are based on a strain amplitude of $\Delta\varepsilon_{eq} = 0.5\%$.

For the purpose of yield surface measurements, starting from a fixed point on the hysteresis curve in the middle of the actual elastic area, different straight strain paths were taken right into the plastic region and the resulting stress values were determined. Then the equivalent stresses were plotted against the equivalent strains in which all measured values were referred to the starting point of the measurement on the hysteresis curve. The equivalent stresses and equivalent strains were calculated using von Mises criterion. From these diagrams yield surfaces with plastic offset strains between 0.01% and 0.5% were determined by a parallel shift of the elastic straight line. For every strain path a new specimen was taken.

3 Results

3.1 *Dislocation structures*

In the case of the Al–3Mg alloy the dislocation structure after a few cycles at the beginning of the fatigue experiment consists of walls which are oriented parallel to {111}-planes. The walls are built of edge dipoles and prismatic loops. Between the walls screw dislocations are moving on favourably oriented {111}-planes.

Depending on the strain amplitude and on the type of loading the dipolar walls change their orientations during the transition into the saturation state. After proportional loadings at $\Delta\varepsilon_{eq} = 0.5\%$ and when the stabilized condition is reached, nearly all walls can be indexed crystallographically following the model of Dickson *et al.* (7, 8). Then, in most cases, two slip systems are responsible for the construction of a given wall. During the process of orientation change, most of the dipolar loops are compressed into new walls by the edge parts of the slip dislocations. These new walls are as accurately as possible perpendicular to both slip directions and the long segments of the loops make acute angles with the walls. In the case of proportional loadings at $\Delta\varepsilon_{eq} = 0.5\%$, {100}-walls dominate in the saturation state, because under those conditions an adequate number of slip systems is activated and the loading directions remain unchanged during the whole experiment. Figure 1(a) gives an example for push/pull loading at $\Delta\varepsilon = 0.5\%$. The dipolar walls are present in a labyrinth of (100)- and (021)-orientations. In Fig. 1(b) only one wall orientation $(11\bar{3})$ is present.

In the case of non-proportional loading the $\Delta\varepsilon_{eq} = 0.5\%$ the {111}-wall orientations from the beginning of the fatigue experiment remain unchanged in most of the grains, even in the saturation state. Because the stress vector is rotating, a fixed slip direction, which is necessary for the reorganization of the walls, does not exist. Further, the number of activated slip systems is higher than in the case of proportional loading and so the possibility of dislocation reactions is also higher. That is why the structures after non-proportional loading become more stable. In Fig. 1(c) a typical example of such a structure is shown. The walls are only weakly condensed, they lie parallel to {111}-planes and consist of prismatic loops besides dislocation nodes. But screw dislocations can also be observed between the walls. Labyrinth structures rarely occurred after non-proportional loading. As an example, the walls in Fig. 1(d) are parallel to (100) and (001).

The dislocation structures after proportional loading must be described as anisotropic, because in most of the investigated grain interiors less than five slip systems were activated. (For reasons of compatibility at least five slip systems

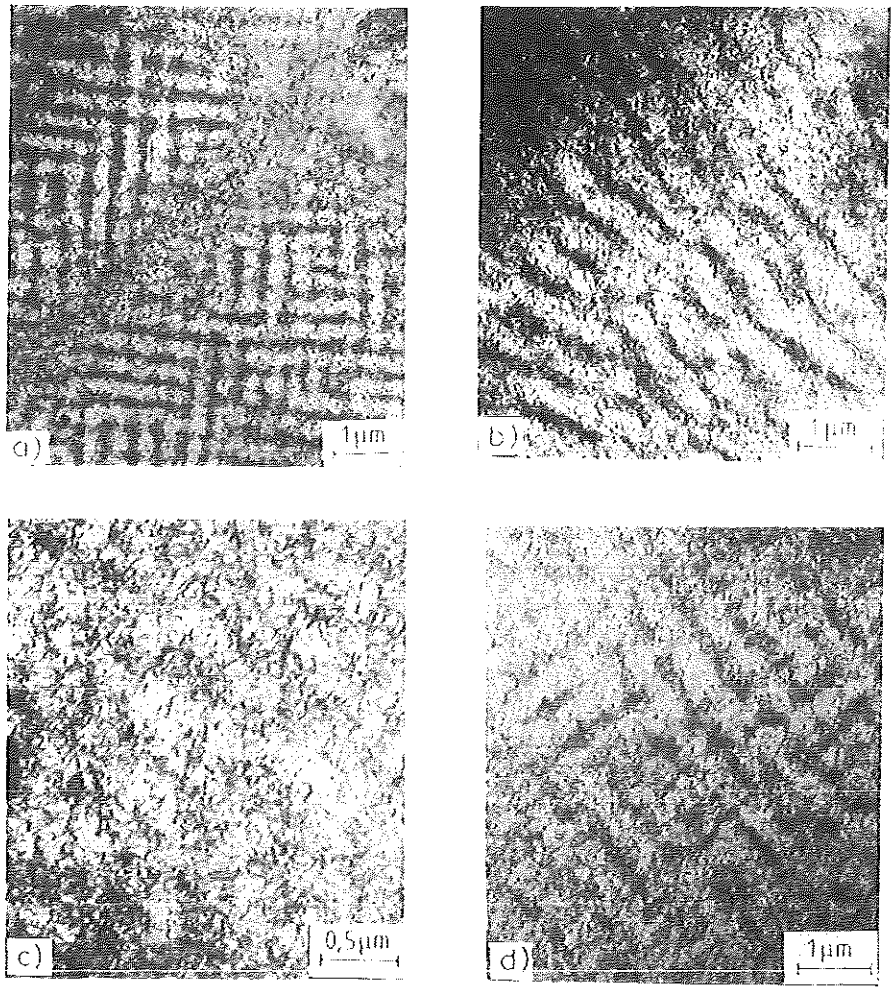

Fig 1 Al–3Mg microphotographs; (a) push/pull, $\Delta\varepsilon = 0.5\%$, stabilized condition (800 cycles), $\bar{Z} = [001]$, $\bar{g} = [200]$; horizontal dipolar walls in (200)-orientation, vertical dipolar walls in (021)-orientation; zone of localized slip parallel to $(11\bar{1})$; (b) push/pull, $\Delta\varepsilon = 0.5\%$, stabilized condition, $\bar{Z} = [1\bar{1}0]$, $\bar{g} = [11\bar{1}]$, dipolar walls in $(11\bar{3})$-orientation; (c) 90° phase shift between push/pull and alternating torsion, $\Delta\varepsilon_{eq} = 0.5\%$, stabilized condition, $\bar{Z} - [01\bar{1}]$, $\bar{g} = [\bar{1}11]$, walls parallel to {111}-planes; (d) 90° phase shift between push/pull and alternating torsion, $\Delta\varepsilon_{eq} = 0.5\%$, stabilized condition, $\bar{Z} = [011]$, $\bar{g} = [1\bar{1}1]$, dipolar walls in (001)- and (100)-orientations.

are necessary. That is why the slip systems often change in the neighbourhood of grain boundaries.) Further, in many grains only one wall orientation was found, see Fig. 1(b). On the other hand the dislocation structures after non-proportional loading are clearly more isotropic.

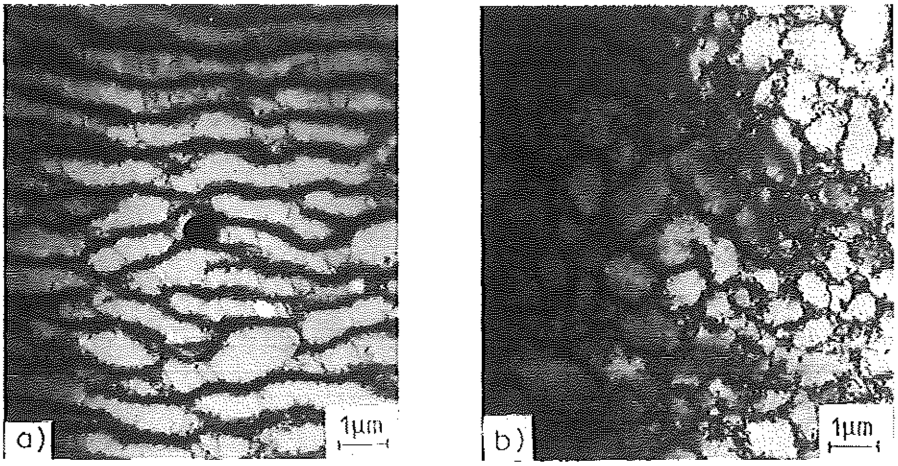

Fig 2 Copper photomicrographs: (a) push/pull, $\Delta\varepsilon = 0.5\%$, stabilized condition (100 cycles), $\bar{Z} = [011]$, $\bar{g} = [1\bar{1}1]$; (b) 90° phase shift between push/pull and alternating torsion, $\Delta\varepsilon_{eq} = 0.5\%$, stabilized condition, $\bar{Z} = [011]$, multibeam condition.

Mainly after proportional loadings the dipolar wall structure can be destroyed parallel to a favourably oriented $\{111\}$-plane. The dipolar loops in these small zones of localized deformation are arranged in bands parallel to that $\{111\}$-plane. In this manner the obstacles in the way of the slip dislocations built up by the prismatic loops become as small as possible. In the deformation bank of Fig. 1(a) only the slip dislocations are in contrast, which have high screw portions in this example.

In the case of copper, after proportional loadings at $\Delta\varepsilon_{eq} = 0.5\%$, the dislocation structure consists of dipolar elongated cells with screw dislocations between the walls, Fig. 2(a). After non-proportional loading with the same amplitude we observed nondipolar isotropic cells with nearly dislocation-free interiors, Fig. 2(b). As known from the literature, after push/pull loading, such structures occur only for larger strain amplitudes (9).

3.2 *Yield surfaces*

First some definitions should be noted: All yield surfaces which were measured after proportional loadings will be called *proportional yield surfaces*. Correspondingly all yield surfaces measured after non-proportional loading will be called *non-proportional yield surfaces*. The diameter in the direction of the preceding alternating load will be described as the *longitudinal value* of a proportional yield surface and the maximum diameter in the direction perpendicular to the preceding alternating load in $\sigma - \tau$ diagram will be called the

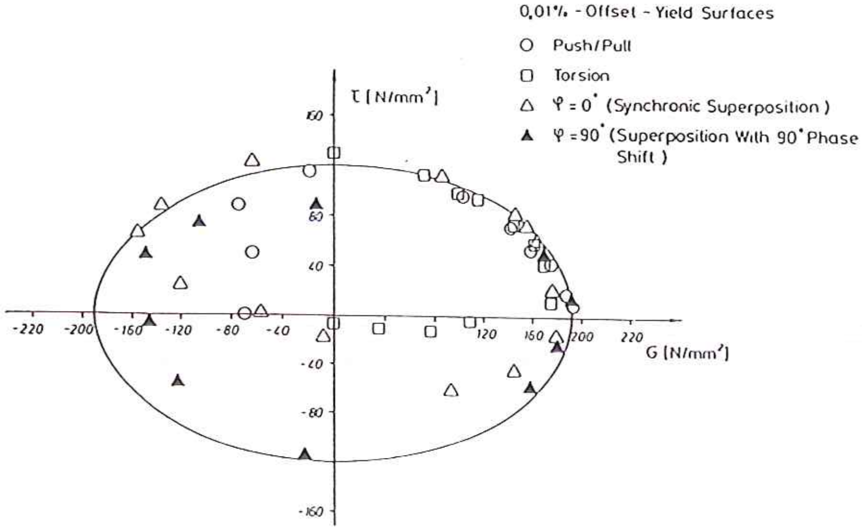

Fig 3 Al–Mg hysteresis curve, $\Delta\varepsilon_{eq} = 0.5\%$, stabilized condition; yield surfaces measured with 0.01% plastic offset strains.

cross value of an proportional yield surface. So the longitudinal value of a push/pull yield surface is its diameter on the σ-axis and its cross value is the maximum diameter of the surface in a direction parallel to the τ-axis. On the other hand the longitudinal value of a torsional yield surface is its diameter on the τ-axis and its cross value is the maximum diameter of the surface parallel to the σ-axis.

As observed in Figs 3 and 4, the proportional yield surfaces of Al–3Mg and of copper, which were measured with 0.01% plastic offset strains at the top of the hysteresis curves, are all flattened in the respective directions of unloading compared with a von Mises-shaped ellipse. So these yield surfaces are anisotropic because their cross values are higher with respect to their longitudinal values than is expected from the von Mises condition. The shape of all proportional yield surfaces becomes elliptical in the zero stress points of the stress/strain-loops but their longitudinal and their cross values remain unchanged (**6**).

The corresponding non-proportional 0.01% offset–yield surfaces drawn in Figs 3 and 4 are larger in the directions in which the proportional yield surfaces are flattened. So the non-proportional yield surfaces are clearly more isotropic than the proportional ones. In the case of copper the non-proportional yield surface is also larger as a whole.

The yield surfaces measured with high offset strains are all isotropic to a great extent (Figs 5 and 6). In the case of copper the non-proportional yield surface is again clearly larger than the corresponding proportional ones.

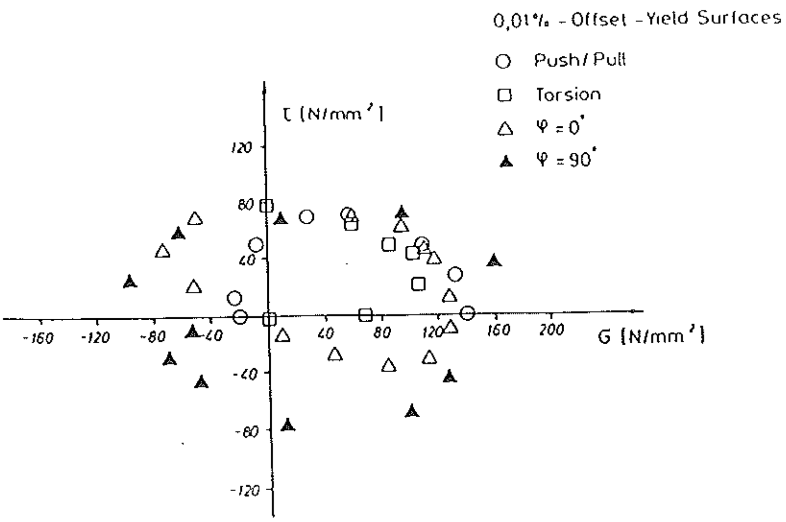

Fig 4 Copper hysteresis curve, $\Delta\varepsilon_{eq} = 0.5\%$, stabilized condition; yield surfaces measured with 0.01 % plastic offset strains.

3.3 *Sequence effects and discussion of the yield surface measurements*

As is well known the Bauschinger effect is the decrease of the yield stress after turning back the loading direction. This decrease can be the result from a shift of the yield surface as a whole and/or a deformation of the yield surface, for example the flattening of the proportional yield surfaces which was observed here. This chapter will discuss whether the flattening of the proportional yield surfaces results from internal stresses or from the anisotropy of the dislocation structure. In the second case the Bauschinger effect can be described only by a shift of the yield surface (kinematic hardening).

On Al–3Mg and on copper the effects of changes in the loading direction from push/pull to alternating torsion (and vice versa) were investigated. Thus the yield surface diameters, which can be taken from the stress/strain loops and the stress amplitudes, were analysed in the transition from the previous to the new saturation state. The equivalent amplitude of total strain was chosen in all cases as $\Delta\varepsilon_{eq} = 0.5\%$. After reversing the load at the point $\sigma(\varepsilon = 0)$ or $\tau(\gamma = 0)$ in a first step, the sample was unloaded to $\sigma = 0$ or $\tau = 0$. Then the cyclic loading in the new direction was started. In this way, before the change, the centers of the yield surfaces were always lying in the origin of the σ, τ-plane.

In this paper only changes from push/pull to alternating torsion are treated. For the reversed direction equivalent conclusions can be drawn.

In Fig. 7 for Al–3Mg and for copper the 0.01 % offset yield surface diameters taken from the torsional hysteresis curves are plotted against the number of

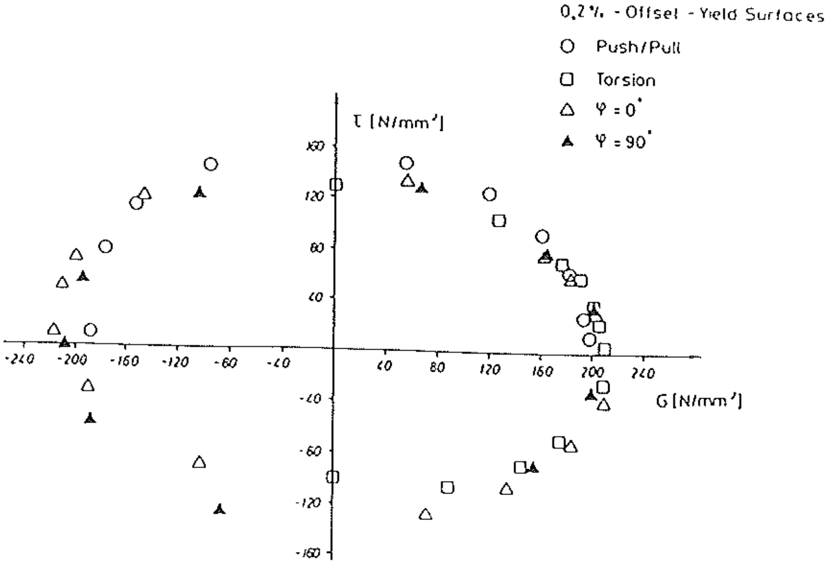

Fig 5 Al–3Mg hysteresis curve, $\Delta\varepsilon_{eq} = 0.5\%$, stabilized condition; yield surfaces measured with 0.2% plastic offset strains.

cycles. The dashed lines correspond to the cross values of the push/pull–saturation yield surfaces and the unbroken lines correspond to the longitudinal

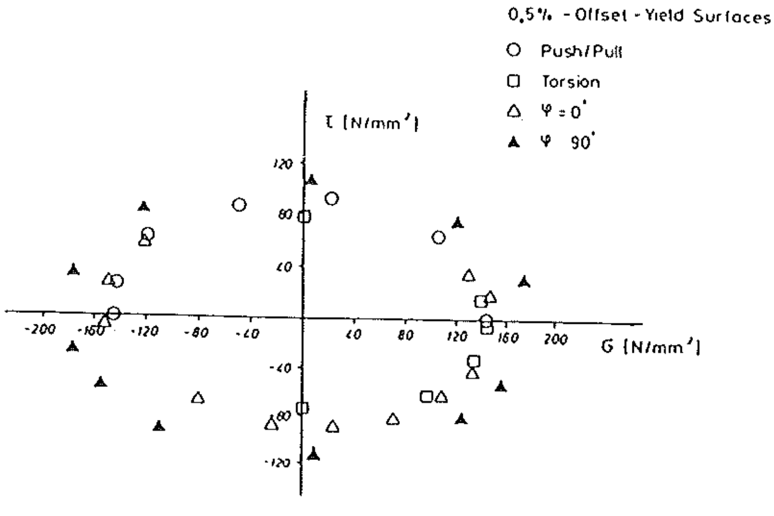

Fig 6 Copper hysteresis curve, $\Delta\varepsilon_{eq} = 0.5\%$, stabilized condition, yield surfaces measured with 0.5% plastic offset strains.

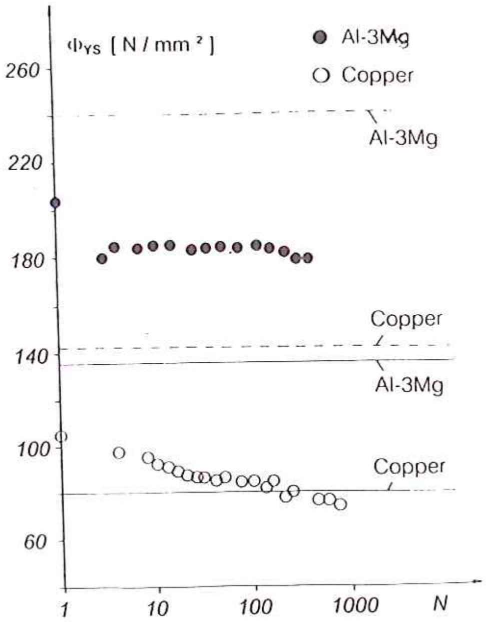

Fig 7 Al–3Mg and copper, 0.01% offset yield surface diameters after the change in loading direction from push/pull to alternating torsion (the broken and unbroken lines are explained in the text).

values of the saturation yield surfaces measured after pure alternating torsion. In Fig. 8 the same evaluation was made for the stress amplitudes of the torsional hysteresis curves after the change of the loading direction. In this case for both materials the broken lines correspond to the initially measured stress amplitudes in torsion after the change and the unbroken lines represent the saturation stress amplitudes of the pure alternating torsion experiments.

By interpreting the flattened regions of the small offset proportional yield surfaces shown in Section 3.2 as the effect of residual stresses, it is to be expected that already in the first cycle after the change in the loading direction, the cross values of the push/pull yield surfaces convert into the longitudinal values of the torsional yield surfaces measured after pure alternating torsion. As can be seen in Fig. 7, this is neither the case for Al–3Mg, nor for copper. The curves for Al–3Mg in Figs 7 and 8 will be discussed first.

According to Fig. 7 (Al–3Mg) the yield surface diameters in fact decrease drastically and rapidly they reach their saturation state but they stay clearly above the longitudinal value of the pure torsion saturation yield surface. Either residual stresses cannot build up to the same extent as in the case of pure alternating torsion, or, after a preceding push/pull loading the saturation yield surface diameter in the torsional direction turns out to be larger in the sense

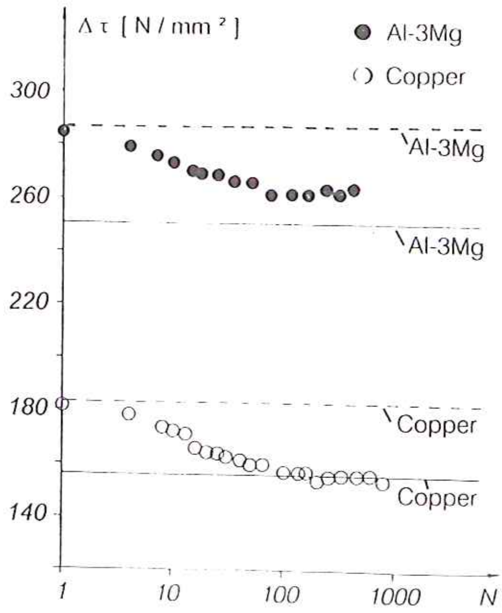

Fig 8 **Al–3Mg and copper, torsional stress amplitudes after the change of loading direction from push/pull to alternating torsion (the broken and full lines are explained in the text).**

of isotropic hardening than the corresponding diameter after pure alternating torsion.

The second case can be interpreted from the dislocation structure. As explained in Section 3.1, in the case of Al–3Mg the dislocation structure after proportional cyclic loadings is anisotropic in the saturation state because in wide areas of the grains only a few slip systems are activated and because the dipolar walls are mostly built up in only one or two crystallographic orientations. During push/pull-loading in a given grain, other slip systems are activated than would be the case in the same grain during alternating torsion. In the same sense, the dipolar walls are built up in such crystallographic planes that the channels between the walls are favourably oriented for the respective direction of alternating load. The screw dislocations move in the dislocation-sparse channels in which – depending on the direction of alternating load – different slip directions and slip planes are preferred in a randomly chosen grain.

If a push/pull experiment is followed by a torsion test, first the dislocation structure is extremely unfavourable for torsion. In the first step the sources of torsional slip dislocations must be activated, in the next step the dipolar walls must change their orientations. As concluded from the curve for Al–3Mg in Fig. 7, most of the torsional slip dislocations are activated during the first three cycles after the change of the loading direction from push/pull to alternating torsion, which results in a dramatic decrease of the yield surface diameter in the torsional direction. When the further reorganization of the dislocations, however, appeared to be hindered, the diameter remains constant during all following cycles. The dislocation structure expected after pure alternating torsion obviously cannot be built up if a push/pull loading preceded. Presumably this is a result of a higher number of activated slip systems after the change in loading direction. To the already existing push/pull dislocations torsional dislocations are added. Moreover the reorganization processes may be hindered by friction as a result of dynamic strain ageing.

After the change in the loading direction, the activation of the first torsional slip dislocations has no influence on the torsional stress amplitude. It is reduced only a little during the first torsional cycles after the change. Probably if the plastic deformation is large enough, in each case the major part of slip is carried by the dipolar walls. These do not change their orientations in the first few cycles to such an extent, that the saturation state for the torsional stress amplitude could not be reached as early as the saturation state of the 0.01% offset yield surface diameters after the directional change of the load. It follows from Fig. 8 that the reorganization of walls, which is significant for the torsional stress amplitude, is completed only after 100 cycles. This reorganization however has no further influence on the 0.01% offset yield surface diameters. It also follows from Fig. 8 that the values of the torsional stress amplitude of the sample subject to the change of loading direction also stay above the saturation stress amplitude of an equivalent pure alternating torsion experiment. Al–3Mg at this point behaves exactly like materials with planar slip (**10**).

The curves for copper determined from the same experiments basically differ from the Al–3Mg results in that the 0.01% offset torsional saturation yield surface diameters as well as the saturation torsional stress amplitude values do not depend on the loading history (Fig. 7 and Fig. 8). In contrast to Al–3Mg, in the case of copper the dislocation structure can be reorganized completely after a change in the loading direction. This behaviour is typical for wavy slip materials like copper (**10**). As a reason one may consider that during proportional loading in copper from the beginning more slip systems are activated than in the case of Al–3Mg. Further cross-slip of the screw dislocation parts may be easier in the case of copper. So for copper the annihilation processes necessary for the change of the dislocation structure can take place. Naturally, in the case of pure copper, the influence of frictional stresses is lower than in the case of Al–3Mg.

Since for the purpose of yield surface measurements the loading direction will also be changed, for the interpretation of the measured yield surfaces one may conclude that:

(1) All yield surfaces belonging to high offset strains are isotropic to a great extent, because during the measuring process for the chosen strain path

sufficient favourably orientated slip systems are activated. At the same time the dipolar walls take complete part in the process of slip. In this way the wall orientations lose significance. Everywhere small deviations from the von Mises condition occur. The non-proportional high offset strain yield surfaces of copper are bigger than the corresponding proportional ones because, in the case of non-proportional loading, easy movable screw dislocations between the walls are missing and the walls themselves have higher strength because they are nondipolar in nature.

(2) The cross values of the proportional yield surfaces measured with small offset strains are clearly larger compared with their corresponding longitudinal values, as expected from the von Mises condition because the plastic offset strain is so small that during the measuring process no additional slip systems are activated. The existing screw dislocations and dipolar walls are unfavourably oriented for the respective cross direction, but for the respective longitudinal direction (direction of the preceding alternating load) they are favourably oriented.

(3) During non-proportional loading more slip systems are activated and the wall formations are more isotropic. For the dislocation motion one can find neither particularly favoured nor unfavoured directions. So the shapes of the yield surfaces turn out to be more elliptical than in the case of proportional loading. In the case of copper, smallest offset strains must even be carried by slip processes in the walls because screw dislocations in the cell interiors are missing. Because of this, in the case of small offset strains, copper also shows significantly larger yield surfaces for non-proportional than for proportional loading.

To support the hypothesis that the shortened longitudinal values of the small offset strain yield surfaces are not caused by the influence of internal stresses, copper samples as well as Al–3Mg samples were unloaded from different points within a torsional saturation cycle. To have the same starting conditions for every unloading condition between two experiments of this kind several full cycles were applied. The half cycles of unloading were analysed in the proven way.

In Fig. 9 the yield surface diameters for both materials taken from the unloading half cycles are plotted as a function of the strain values from which the unloading had taken place. For a given offset strain for both materials at every point of the respective stress/strain loop the same longitudinal values of the yield surfaces were measured. If an influence of internal stresses existed, one would expect increasing longitudinal values of the yield surfaces in the zero stress points of the hysteresis curves because in these points the back stresses vanish.

4 Summary and Conclusions

In the case of Al–3Mg the dislocation structures found after proportional alternating loadings at $\Delta\varepsilon_{eq} = 0.5\%$ were walls consisting of dislocation dipoles.

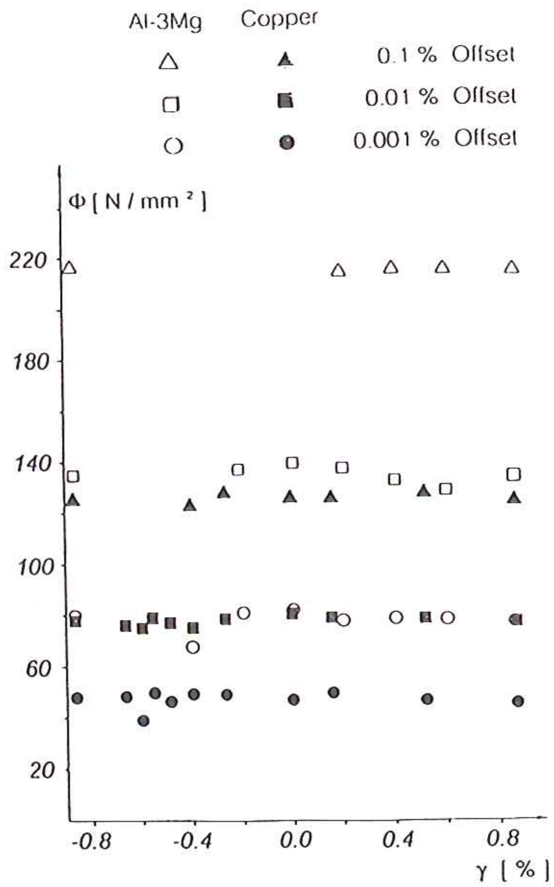

Fig 9 **Al–3Mg and copper, change of yield surface diameters, measured in the direction of alternating load, during a torsional cycle.**

Between the walls, screw dislocations as slip dislocations were observed. The crystallographic orientations of the walls could be determined after a model of Dickson.

The dislocation structures observed after loading with 90° phase shift between push/pull and alternating torsion were mainly (111) walls consisting of dipoles and dislocation nodes. Because the dislocation walls after proportional loading only exist in one or two different orientations, these structures are anisotropic. In contrast the dislocation structures after non-proportional loading are clearly isotropic.

In the case of copper after proportional loadings at $\Delta\varepsilon_{eq} = 0.5\%$ elongated dislocation cells consisting of dipols were found. Also here screw dislocations as slip dislocations lie between the walls. After non-proportional loading only isotropic cells, nondipolar in character, were built up.

Compared to von Mises ellipses the proportional yield surfaces measured in the tops of the stress/strain loops are flattened in the respective directions of unloading. So their cross values are larger in comparison with their longitudinal values than could be expected from the von Mises condition. From this point of view the proportional yield surfaces are anisotropic. In contrast the non-proportional yield surfaces are clearly more isotropic and in the case of copper they are significantly larger.

It can be concluded from experiments in which the loading direction was changed from push/pull to alternating torsion that the anisotropy of the proportional yield surfaces can be explained by the anisotropy of the dislocation structure. The flattening of proportional yield surfaces can not result from internal stresses because their longitudinal values remain constant during one cycle (see Fig. 9). So the Bauschinger effect can only be described by a displacement of the yield surface as a whole (kinematic hardening). Nevertheless by an extension of the simulation models from one axial to multiaxial conditions, the changings in the shapes of the yield surfaces must be taken into account.

References

(1) DAFALIAS, Y. F. and POPOV, E. P. (1976) Plastic variables formalism of cyclic plasticity, *J. Appl. Mech.* 645.

(2) McDOWELL, D. L. (1986) A two surface model for transient non-proportional cyclic plasticity, part 1; Development of appropriate equations, *J. Appl. Mech.*, **85**, 298.

(3) ELLYIN, F. (1989) An anisotropic hardening rule for elastoplastic solids based on experimental observations, *J. Appl. Mech.* **56**, 499.

(4) GUPTA, N. K. and LAUERT, H. A. (1983) A study of yield surface upon reversal of loading under biaxial stress, *Z. angew. Math. u. Mech.*, **63**, (10), 497.

(5) WILLIAMS, J. F. and SVENSSON, N. L. (1971) Effect of torsional prestrain on the yield locus of 1100-F aluminium, *Journal of Strain Analysis*, **6**, (4), 263.

(6) GIESEKE, W. (1995) Fließflächen und Versetzungsstrukturen metallischer Werkstoffe nach plastischer Wechselbeanspruchung, Dissertation, TU Braunschweig, Germany.

(7) DICKSON, J. I., BOUTIN, J. and L'ESPERANCE, G. (1986) An explanation of labyrinth walls in fatigued FCC metals, *Acta Metall.*, **34**, (8), 1505.

(8) DICKSON, J. I., HANDFIELD, L. and L'ESPERANCE, G. (1986) Geometrical factors influencing the orientations of dipolar dislocation structures produced by cyclic deformation of FCC metals, *Master. Sci. Eng.*, **81**, 477.

(9) FELTNER, C. E. and LAIRD, C. (1967) Cyclic stress–strain response of FCC metals and alloys–II dislocation structures and mechanisms, *Acta Metall.*, **15**, 1633.

(10) FELTNER, C. E. and LAIRD, C. (1967) Cyclic stress–strain response of FCC metals and alloys–I phenomenological experiments, *Acta Metall.*, **15**, 1621.